STUDY OF NAKTONG VALLIS, MARS: SUSTAINED FLUVIAL ACTIVITY EXTENDING DURING THE HESPERIAN PERIOD. S. Bouley[1], V. Ansan[1], N. Mangold[1] , Ph. Masson[1], and G.Neukum[2]; and the HRSC co-Investigator team [1] IDES – University Paris Sud – 91405 Orsay – France; [2] FU Berlin, Germany. (sylvain.bouley@u-psud.fr)

Introduction: Naktong Vallis (Fig. 1) is located on the southern highland plateau on the south of Arabia Terra. This valley is the southern part of a very large valley network [1]. This network composed by Naktong, Scamander and Mamers Valles is one of the longest valley network on Mars with a total length of 4700 km. Naktong Vallis is interesting to study because it represents the upper part of this large valley network. This valley debouched north of Arago crater (10°N, 30°E) and the head is on Terra Sabae (4°S, 38°E). The longest stream of Naktong Vallis has a length of 1200 km and this fluvial network is composed by several tributaries with a medium drainage density.

With the HRSC camera of the mission Mars Express, it is possible to study with precision the morphology of sources and to determine which processes have formed Naktong Vallis. In Arabia Terra, there are the Noachian cratered surface and younger intercrater plains. Activity of fluvial valleys is accepted during the Noachian period (>3.7 Ga) but duration are unknown. We were able to precise when Naktong vallis was active. To know more about the activity of this valley, it is important to study the relationship between the intercrater plains and the valley. Here, we show that the activity was ungoing after the intercrater plains.

Data and methods: The HRSC Camera of Mars Express allows us to study Naktong Vallis with high resolution and large coverage. We used ten nadir HRSC images with a resolution between 10 and 15 m/pixel that we mosaiced to study the whole fluvial network. We identified and mapped valley network and define the drainage basin and determine the different properties of Naktong Vallis like stream length, density and Strahler order. HRSC images were useful to analyze the morphology of head and the valley. Additionally, we used digital topography from MOLA at a resolution of 460 m/pixel. MOLA topography allowed us to observe longitudinal and cross-section profiles of the valley. We can also examine the morphology of different tributaries and observe the variation of different parameters like local and regional slope in the valley. With the MOLA data, we realise the roughness map with the technique described by Kreslavsky et al [2]. This map was useful to put intercrater plains forward. We were able to also see easily the relationship between plains and the valley.

Major characteristics of Naktong Vallis: *Network geometry:* Figure 1 shows our analysis for the drainage composition of Naktong Vallis. For each mapped valley, an order is allocated with the Strahler method [5] and is indicated its relative importance in the network. Naktong Vallis is a fifth-order system included 383 segments with a total length of 4616 km. Carr [3] determined in 1995 with Viking data (200 m/pixel) a drainage density for Naktong Vallis equal to 7.6×10^{-3} km^{-1}. With a global mapping of this valley with HRSC images, we found a drainage basin with an area of 2.7×10^{5} km² and a drainage density equal to 1.7×10^{-2} km^{-1}. This value is larger than the one proposed by Carr but is smaller than the one equal to 6.5×10^{-2} km^{-1}proposed by Hynek et al [4]. Carr used Viking data with a lower resolution than HRSC images and Hynek mapped valleys with MOC wide angle images in some regions where there were no valleys to observe. This network is one of the largest on Mars but has finally a medium drainage density when you compare this network with others like in Aeolis region [6] or Warrego Vallis [7] which have drainage density up to 0.1 km^{-1}. Different processes of formation could be at the origin of these different values. We found a constant bifurcation ratio (R_b) equal to 4.16. This value is consistent with terrestrial R_b values which are between 3 and 5 [8]. The mean length ration R_l is equal to 3.8 and is consistent with terrestrial values (1,5-3) [8]. Nevertheless R_b and R_l are empirical and have no physical meaning on Earth.

- *Topographic parameters:* With MOLA data we observed that Naktong Vallis has an important difference of altitude between its head and its mouth. The highest point is at 1800 m (Fig.2) and the mouth is at -1000m. Irwin et al. [1] show that the mean slope for the network Naktong, Scamander and Mamers Valles is around 0.1°. Figure 2 shows the longitudinal profile from heads until the point E (3°N, 34°E). The noisy profile with variations of more and less 50 meters can be explained by a lot of landslides on valley's sides. We observed that the mean slope value is valid after the Chaos but segments A-D, B-Chaos and C-D has different slopes. We observed 2 larger values for segments A-D and B-Chaos with slopes respectively equal to 0.25° and 0.16° and one almost identical to the mean slope for the segment C-D. Segment C-D is more dendritic with small streams than segments A-D and B-Chaos.

Morphology of valley and chronology:- *Morphology of valley:* The morphology of the valley on HRSC images shows that the profile is rectangular with high slope sides and a flat bottom.

Figure 3 shows different MOLA topographic cross-sections along the valley from the head until the mouth. Profiles are not rectangular because MOLA data have a low resolution and we don't have enough measure points to resolve valley's sides. We observed that the valley has a constant width along the valley around equal to 4 km. This wide valley from the head is representative of valley formed by sapping. Despite the low resolution of MOLA Data, it is possible to know the depth of the valley because of its large width. The depth of the valley increases with the distance to the head (Fig. 3). Near the head, depth is around 100 m and near the mouth, depth is between 200 and 300 m. There is more and more erosion far from heads; this could be the result of increasing discharge rate.

- *Morphology of sources:* The three HRSC images on figure 4 show three heads of Naktong Vallis. Even if the morphology is not exactly the same because of their different dentritic features, we observed that heads display large amphitheatres for each case. This morphology is peculiar to sapping process. Sapping is caused by subsurface groundwater and backward erosion. The width of the valley is large from its head with typically 1 km on figure 4. Heads look to be only in flat and smooth terrains which are intercrater plains.

- *Intercrater plains and chronology:* In Naktong region, we observed a lot of intercrater plains. These plains are certainly composed of a deposit of horizontally layered material [9]. We mapped these plains in using HRSC images (fig. 4) for the morphology and techniques of Kreslavsky et al [2] for the roughness. In HRSC images, intercrater plains are smooth, flat and there are a lot of wrinkle ridges that can be interpreted as compression ridges [10]. On the map of roughness (fig. 3b), intercrater plains are dark. It means that plains have a low roughness that can be consistent with the smooth terrains observed with HRSC that could be interpreted as sediment or volcanic deposits.

On the figure 1, Naktong Vallis has three different relationships with intercrater plains. On terrains 1, 2 and 3 (fig.1 and 3), Naktong Vallis has their heads in these plains. Also on terrain 3 (fig. 1), the valley incised intercrater plains along more 200 km. These two observations mean that the valley was again active after the formation of these plains. On terrain 5 (fig.1), heads seem to be almost on a large intercrater plain but they stop before. This large plain might have been eroded close the heads and this is the reason we can't observe smooth plains just around heads. On terrain 4 (fig. 1), intercrater plains cover Naktong Vallis but we observed low incisions on plain sides. The formation of this plain ends certainly the activity of Naktong Vallis for a time but activity existed again after the plain's formation. Nevertheless it's difficult to say how long the activity continued after the deposit of terrain 4. We are in presence of two intercrater plains with two different ages and it is interesting to try to date these different plains. Using Hartmann and Neukum Mars cratering chronology model [11], it is possible to date intercrater plains. For four different plains (table 1), we found values for N(1) including uncertainties between $2.8.10^{-3}$ and $4.8.10^{-3}$ crater.km^{-1}. Despite uncertainties, these densities corresponds to the Hesperian period defined by N(1) value between $1.6.10^{-3}$ and $6.5.10^{-3}$ crater.km^{-1} [11]. For many authors [1][3][12], fluvial network have been formed during the Noachian but our study proved that Naktong Vallis was active or at least reactivated during the Hesperian period. The different plains observed with HRSC images has certainly not the same age but it is not possible to measure this difference in counting craters because of the high uncertainties which exists on the absolute age determination.

Conclusion: Naktong Vallis with its rectangular valley and heads in amphitheatres and its medium drainage density shows that groundwater sapping was certainly a major process, either to form this valley or to reactivate it after the intercrater plain emplacement. We proved that this valley was active during the Hesperian epoch but we don't know if Naktong Vallis formed during that period or if it is the continuity of a noachian activity. To precise the duration of activity, it will important to study probable discharge in this valley and differences of crater filling

References: [1] Irwin III R.P. et al. (2005) *JGR*, 110, E12S15. [2] Kreslavsky M.A. and Head III J.W. (2000) *JGR*, 105, NO.E11, 26695-26711. [3] Carr M.H. (1995) *JGR*, 100, 7479-7507. [4] Hynek B.M. and Philips R.J. (2003) *Geology*, September 2003, 757-759. [5] Strahler A.N. (1952a) *Geol. Soc. Am. Bull*, 63, 898-912. [6] Ansan V. et al (2007) *Geoph. Res. Abstracts*, 9, 09722. [7] Ansan V. and Mangold N. (2006) *Planet and Space Science*, 54, 219-242. [8] Horton R.E. (1945) *Geol. Soc. Am. Bull.*, 56, 275-370. [9] Moore M. (1990), 95,14279-14289. [10] Montési L.G.J and Zuber M.T. (2002), *JGR*, 1-22. [11] Hartmann W.K. and G. Neukum, *Space Sci. Rev.*, 96, 1-30, 2001. [12] Irwin III R.P. and Howard A.D (2004), *JGR*, 109, E12009.

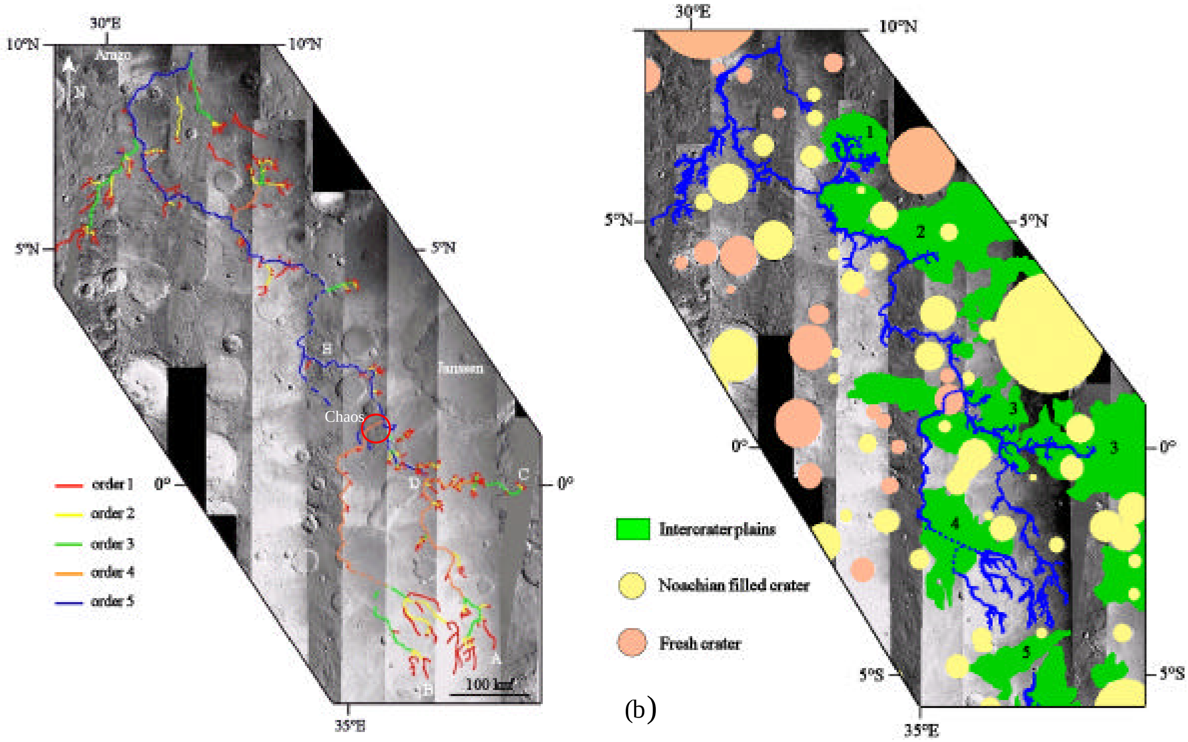

Fig. 1 (a) Map of the Naktong network with Strahler's order and table of the drainage composition. (b) Map of intercrater plains and Noachian filled and fresh crater

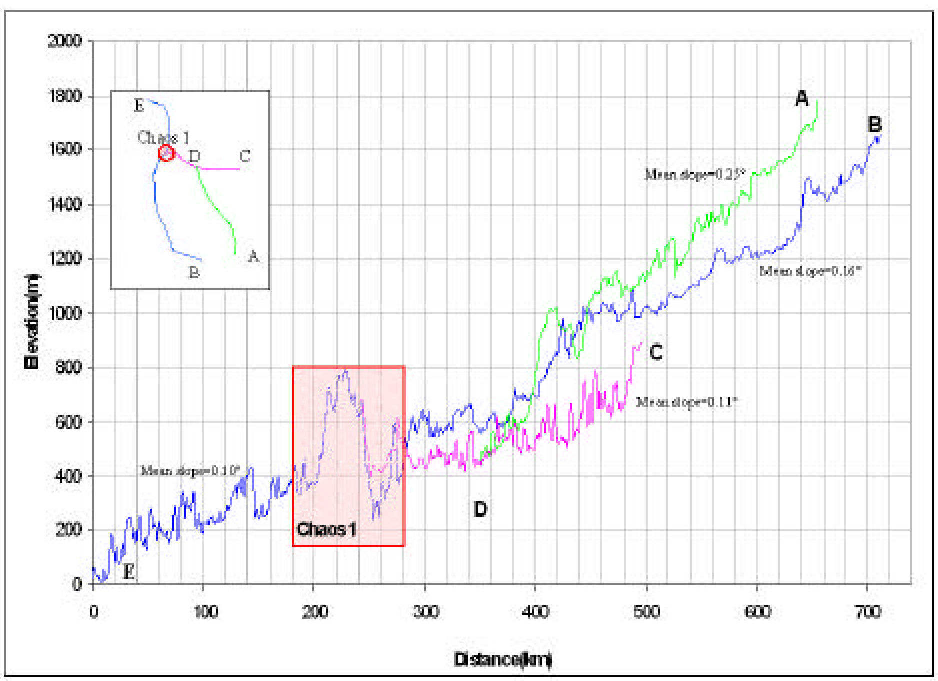

Fig. 2 MOLA Longitudinal profile of Naktong Vallis

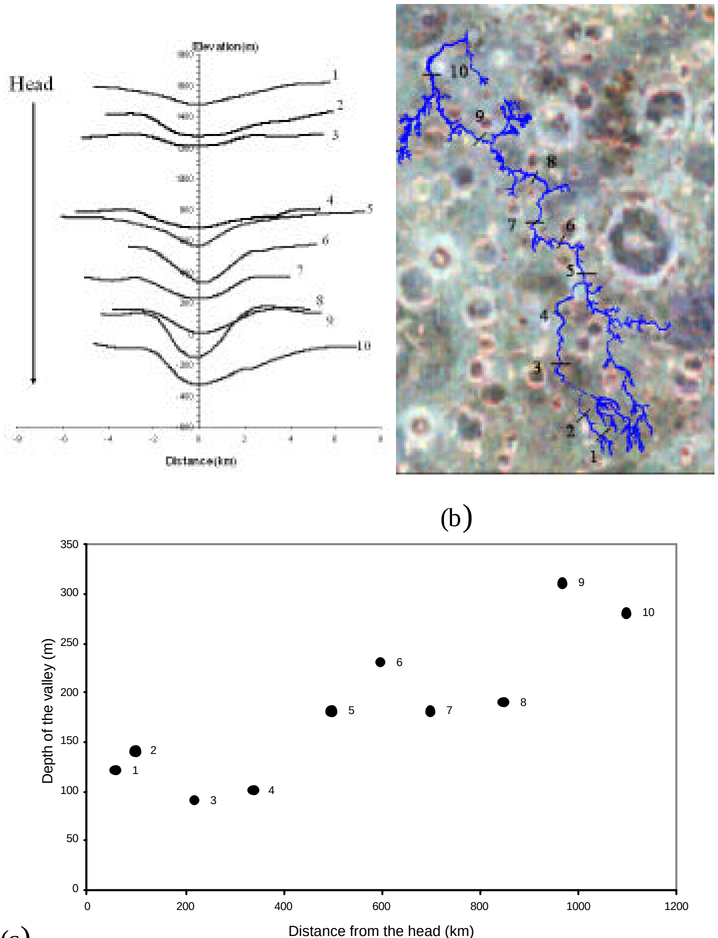

Fig. 3 (a) Variations of sections profiles of Naktong Vallis from the head. (b) Roughness map of Kreslavsky et al [2]. (c) Variations of valley's depth from the head

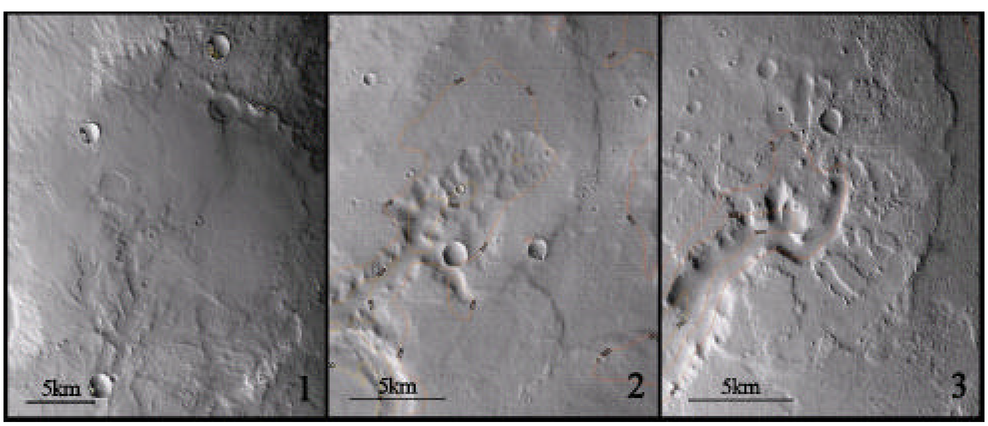

Fig. 4 Three heads of Naktong Vallis in amphitheatres. 1- 7°N;33°E / 2- 4°N;35°E / 0°N;38.5°E

region	A(km²)	N	N(1) (crater/10^6 km²)	N(1) error
1	4152	16	3853	+/- 963
3	17500	71	4057	+/- 481
4	6407	23	3589	+/- 749
5	5565	21	3773	+/- 823

Table 1 N(1) determined by crater count with Hartmann and Neukum model [11].N: number of craters/ A: Area Hesperian period: 1600<N(1)<6500